M. A. Oghabian PhD [1],
N. Riahi Alam PhD [1],
S. Mehdipour MS [2].

A New Method for Measurement of Radio Frequency Inhomogeneity in MRI

Abstract: We introduce a new method of measuring transmit and receive RF inhomogeneity in different RF coils of MRI systems. In this method a single slice of a uniform phantom is imaged from different flip angles, using a standard spin echo protocol. The signal intensity in these images is then fitted to a mathematical model which describes the relationship between the signal intensity and flip angle of the spin echo images. The results of this curve fitting process are two parameters, T(r) and R(r), whose variation with the spatial position shows RF transmit, and receive non-uniformity, respectively.

In this approach a linear profile of B1 field distribution and receive sensitivity of RF coils are achieved which is also applicable *in vivo*. The method can be used to assess any commercial MR scanner and is highly recommended for the quality control (QC) of those MR scanners which are devoid of complicated protocols such as SE(θ-2θ). Such systems are still running in different clinics especially in the developing countries where the latest high performance MR scanners are not available and many scanners lack standard maintenance services.

Keywords: Magnetic Resonance Imaging, RF inhomogeneity, Image non-uniformity, spin echo

Introduction

Image non-uniformity is one of the most important parameters of MR imaging that, can deteriorate the results of quantitative, diagnostic and post-processing studies.[1] Therefore, the quality control (QC) is of absolute importance, particularly for all the old MR scanners not equipped with the new pulse sequences of the recent QC programs. The proposed method could reveal the causes of image non-uniformities due to the main and radio frequency (RF) magnetic field inhomogeneities by providing a simple way of measuring the magnetic field characteristics. This method is highly recommended for most countries like ours where still older MR systems with poor maintenance are used.

As claimed by a number of researchers, the RF field inhomogeneity is one of the most important causes of image non-uniformity.[2-4] The RF field inhomogeneity has two distinct causes; first an interaction between the RF field and the body being imaged, and second, the inherent inhomogeneity of the RF coil. The inherent RF non-uniformity is attributed to the surface coils, though the so-called uniform volume coils are not perfect either.

Various methods have been introduced to measure the transmitted B_1 and receive sensitivity distributions of RF coils. One method is the direct measurement of the field through measuring the induced voltage in a small pick-up coil.[5,6] This takes a long time and its mechanical system must be designed properly so that the strong static magnetic field would not interfere with its function. In addition, inserting the coil into the RF coil, by itself, disturbs the field homogeneity.

Some other methods are based on the theoretical analysis of the problem; Biot-Savart relation or finite element analysis are the examples.[7-9]

From
1. Tehran University of Medical Sciences, Medical Physics department, Tehran, Iran.
2. Research Center for Sciences and Technology in Medicine, Imam Hospital, Tehran, IRAN.
Corresponding Author:
M. A. Oghabian, PhD,
E-mail: oghabian@sina.tums.ac.ir

When using Biot-Savart equation the main drawback is that the effects of Eddy currents are not considered. Moreover, finite element methods are too expensive and take a long time to work. To avoid the above problems, some methods which use image information for calculating B_1 distribution have been proposed as a substitute.

A number of those methods need specially designed pulse sequences which are not available on all scanners.[10-12] Insko has proposed a method which uses a special kind of SE (θ-2θ) and FE sequences.[13] However, the FE and SE sequences used in their study are influenced by B_0 inhomogeneity. JG Barker also used ten θ-2θ spin echo images.[14]

Stollberger *et al*, designed a special pulse, yet with the same limitations. Thulborn has proposed a very fast method, though, it is not applicable to all commercial scanners, since it uses EPI pulse sequences which require special hardware and software.[15]

Our proposed method is to use a routine θ-180° spin echo pulse sequence. This method can measure receive RF uniformity in a homogeneous sample, and the transmitted B_1 field both *in vivo* and *in vitro*. By varying the flip angle, eleven different images are acquired from a single slice, while all other imaging parameters are kept constant. Signal intensity is measured at different points of these images. The measured data are then fitted to a mathematical model which has been derived from applying the relevant rotation matrices to the magnetization vector. Two functions, T(r) and R(r), are derived from the curve fitting process, which show the RF transmit and receive uniformities, respectively. This method has some similarities to Barker's method but as it uses a θ-180° spin echo, it is less sensitive to B_0 inhomogeneity. Furthermore, when using this pulse sequence, we did not experience those slice profile problems reported before.[14] RF inhomogeneity correction and compensation for B_1 field are essential for computational quantitative analysis of MR images and are widely used for different applications.[16-19] Moreover, devising various RF coils, phantoms and QC procedures is necessary for evaluation of MR imaging systems.[20]

Theoretical Basis for the Proposed Method

If the transmitted B_1 field is non-uniform, then the protons experience different flip angles in the imaged volume. In other words, flip angle will have spatial variation. We show this spatial dependence with a function called T(r). So:

(1) $\quad \theta_{(r)} = T_{(r)}.\theta_0$

where, θ_0 is the nominal flip angle which is set by the operator as an imaging parameter and T(r) is a function of position which shows the flip angle distribution over the volume being imaged. So, we could say T(r) represents B_1 field non-uniformity. If the real flip angle is equal to the nominal flip angle at a spatial position, then T(r) equals one. The less variation in this function, the more uniform the field is. On the other hand, if the sensitivity of the RF system (as shown by R(r)) changes with position, the received signal intensity will change, accordingly. So:

(2) $\quad S_{(r)} = R_{(r)}.S_0$

This means if the real signal intensity equals the nominal value somewhere in the RF coil, then R(r) equals one at the same point. Therefore, the uniformity of these functions is a good measure of the RF receive uniformity.

Spin echo pulse sequences are the best choices for measuring the net RF non-uniformity since they have little dependency on the B_0 inhomogeneity and gradient currents. Moreover, they are common to all commercial scanners, and that is why we have focused on this pulse sequence.

For a θ-2θ pulse sequence we have:[14]

(3) $\quad S_0 = k.\,PD.\,Sin^3\theta$

where, k represents the receiver gain and PD is the proton density of the sample. Combining equations (1) and (2), yields:

(4) $\quad S_{(r)} = k.\,PD_{(r)}.\,R_{(r)}.\,Sin^3(T_{(r)}.\theta)$

The calculations for the signal response of a $\theta x\text{-}\tau\text{-}\alpha y\text{-}\tau$ spin echo pulse sequence can be found in the Appendix. From the equation (A-9), we have:

(5) $\quad S_0 = k.\,PD.\,Sin(\theta).\,(1-Cos(\alpha))$

Therefore, by equations (5) and (4) we could say:

(6) $\quad S_{(r)} = k.\,PD_{(r)}.R_{(r)}.\,Sin(T_{(r)}.\theta_0).\,(1-Cos\,(T_{(r)}.\alpha_0))$

In a routine spin echo pulse sequence, the second RF pulse, a 180° pulse, is responsible for the rephasing process. Therefore:

(7) $\quad S_{(r)} = k.PD_{(r)}.\,R_{(r)}.\,Sin\,(T_{(r)}.\theta_0).(1-Cos(T_{(r)}.\pi))$

As was mentioned above, θ_0 is the nominal flip angle chosen by the operator. Note that the RF transmit

non-uniformity, if present, affects all the pulses in a sequence, and hence, both the θ and 180° pulses are affected. That is why we did not give a 180° value to the second pulse (αy) from the beginning, when calculating the signal response. It is clear that in the above equation of the transmit non-uniformity function (T(r)) affects the second flip angle as well.

Materials and Methods

All our experiments were performed by a Picker VISTA HPQ 1.5 T MRI scanner. A cylindrical Perspex phantom of 25.5 cm in length and 24.0 cm in diameter was used as the uniform sample. The phantom was filled with liquid vegetable oil. The main advantage of using oil phantom for this study is that the skin depth effect and standing waves have little effect on RF inhomogeneity. This is due to the fact that oil has a small electric permittivity (ε_r=5) and its conductivity is low too.[7]

According to equation (7), for determining T(r) and R(r) and investigating their variations, a number of images with different nominal flip angles (θ_0) are acquired. At a particular spatial position (r) the signal intensity is measured for all of the images and is plotted against the nominal flip angle. The data, then were fit to equation 7, and the two parameters T(r) and k.PD(r).R(r) are determined for that position. This process is repeated for all other positions. At a reference point, the two functions T(r) and R(r) are supposed to have a value of one. Doing so, the value for k.PD(r) was determined. Provided that all of the images are acquired from a uniform object, with the constant proton density function, the value of R(r) can be determined if k is constant for all the images. Plotting T(r) and R(r) *vs* the spatial position (r) will give us the RF transmit and receive characterizations of the relevant RF coil. In cases that proton density function (PD(r)) is not constant (*e.g.*, situations *in vivo*), R(r) function is not measurable, however T(r) can still be determined.

The first point to be noted is that to have a complete relaxation and to avoid saturation, the used TR should be large enough with respect to the sample's T_1. On the other hand, for a short study time, TR is desired to be short. Considering both these limitations, a TR of 1000 ms was used for the current study. TE does not directly affect the results, but it should be noted that if TE is chosen to be too long, the signal intensity and hence the signal-to-noise ratio, decreases. In such situation, noise will dominate the images. With TE=60, noise is kept fairly low and S/N is over 80 for all the images. Signal intensity variations due to RF field non-uniformity is of a smooth nature, thus we do not have to use fine image matrices that increase both the image file size and the image acquisition time. Procedures such as shimming, RF scaling and center frequency adjustment, were all performed automatically by the system. The image gain was set manually and was kept constant for all the taken for each study.

As mentioned earlier, for each study, eleven images with different flip angles of 10, 20, 40, 60, 80, 90, 100, 120, 140, 150, and 160° were obtained. To investigate the capability of this method to detect possible transmit and receive RF non-uniformity, a virtually non-uniform condition was required. We will certainly have receive RF non-uniformity when using surface coils. However, for transmitting RF, this system only uses 16-column birdcage volume coils (head and body) which usually maintains good uniformity inside their imaging volume. Therefore, for simulating non-uniform RF transmit and receive conditions, the smaller head coil was used and the phantom was located partially outside the coil. In this way, eleven coronal sections of the phantom were also taken from the above-mentioned flip angles.

Having these images, on all of them, a similar ROI was selected along the central axis of the oil phantom and their mean signal intensity was read. A least squares curve fitting process was then performed (MATLAB, Mathworks Inc) to fit the gathered data to equation 7 and to derive the respective T(r) and R(r). Thereafter, the center of the ROI was moved along the axis of the phantom (the head-to-feet direction) and the same process was repeated.

To investigate the capability of this method to distinguish between RF transmit and receive non-uniformities, a circular surface coil, 10.7 cm in diameter (TM joint coil) was used as the receiver and a birdcage body coil was used as the transmitter. The oil phantom was positioned with its axis orthogonal to the static magnetic field and the receiver coil was put on it longitudinally. Again, eleven images were taken from the same earlier-mentioned flip angles. However, this time, in the trans-axial plane. For these images, ROIs were selected both along the anterior-posterior direction and the axis of the phantom (which is also the axis of the TMJ). Similarly, T(r) and R(r) were calculated via curve fitting. The resultant T(r) described the transmit characteristics of body coil and the calculated R(r) described the receive characteristics of the circular surface coil.

Results and Discussion

The spatial position of each ROI and the output of curve fitting process are shown in Table 1. P(1) and P(2) are the direct output of curve fitting process (P(1)=k.PD(r).R(r)), while R(r) and T(r) are the normalized values for these two functions, respectively .

It is obvious in Figure1 that as we move to ROIs which are further away from the coil center, the respective ROI curve gains a shorter height. Besides, for different curves, the maximum height occurs at different flip angles. As we move to an ROI further away from the coil center, it peaks at larger nominal flip angles. In other words, in this geometry both the transmitted B_1 field and the receive sensitivity decrease as we move further away from the center of the coil.

For a better display of T(r) and R(r) variations, they are plotted against the spatial position r (Figure 2). In this Figure, T(r) and R(r) are marked with '*' and 'o', respectively. As expected, both of the functions decrease when moving away from the coil center, where the transmit and receive non-uniformities are noticeable. Therefore, this method is capable of revealing RF transmit and receive non-uniformities and can be used efficiently.

One of the eleven images which were taken using the TMJ coil—to investigate whether this method was able to distinguish between the RF transmit and receive uniformities—is shown in Figure 3. In this image, the points close to the receiver coil gain higher signal intensities (as expected). A TNG tablet which was used to mark the center of the TMJ coil is shown as a bright spot at the top of the image. ROIs were aligned along the TMJ coil axis, 20 mm apart from each other, and the mean signal intensity was measured on each ROI for each image. As described earlier, the data for each ROI was fitted to equation. (7) and the best fit curves for each ROI were selected as shown in Figure 4. The curve pertaining to the region closest to the receiver coil is marked with '*' and that farthest away is marked with '×'.

As shown in Figure 3, the more distant ROIs from the receiver coil have less height. However, the position for peak signal intensity is almost fixed somewhere between 2 and 2.5 radians. Therefore, in this geometry the transmitted B_1 field produced by body birdcage coil is almost uniform, whereas the receive sensitivity of the TMJ coil varies from one ROI to another and decreases as the distance between the ROI center and the receiver coil increases. In this figure, T(r) is the transmit uniformity of the bird cage body coil in a trans-axial plane, i.e., along the AP direction, and R(r) is the receive uniformity of the TMJ coil along its axis. These two functions are plotted against the spatial position r in Figure 5. In this Figure, the horizontal axis was positioned along the AP direction.

The anterior direction is considered positive and the posterior negative. In this Figure, R(r) is marked with '*' and T(r) is marked with 'o'. As expected, T(r) variation is low while R(r) variation is high. There-

fore, this method distinguishes between the transmit and receive uniformities.

Table1: Results of curve fitting process for different ROIs for images of oil phantom, with the phantom partially outside the head coil. F stands for feet direction with respect to the magnet iso-center.

ROI position	Symbol	P(1)	P(2)	R(r)	T(r)
35.6F	*	2.8669e3	0.8560	1.000	1.000
51.3F	∘	2.6311e3	0.7631	0.9177	0.8915
66.9F	□	2.3894e3	0.6614	0.8334	0.7727
78.6F	△	2.1735e3	0.5853	0.7581	0.6838
90.3F	◇	1.9350e3	0.5087	0.6749	0.5943
105.9F	+	1.5004e3	0.4179	0.5233	0.4882
119.6F	▽	1.3054e3	0.3215	0.4553	0.3756
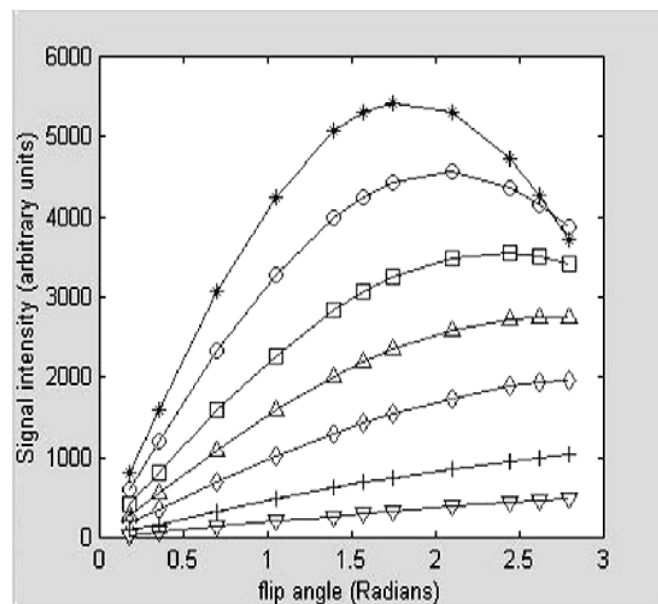
Figure 1: Signal intensity variations vs flip angle for images of the oil phantom, partially outside the head coil. See Table-1 for definition of symbols.
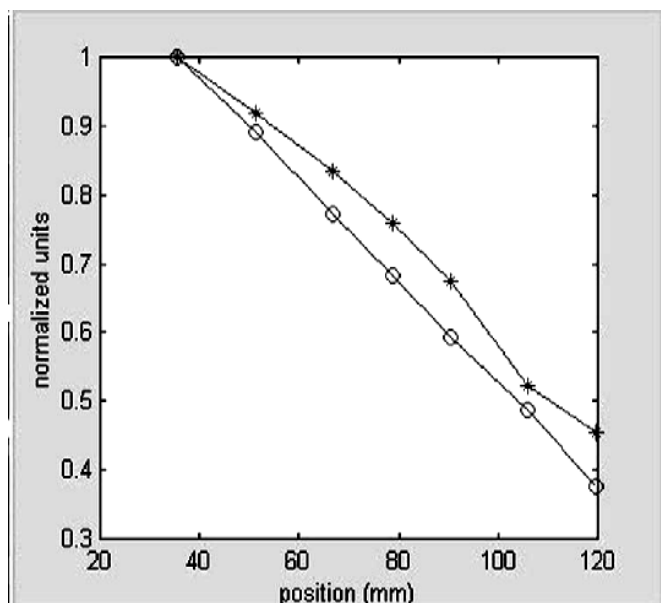
Figure 2: T(r) and R(r) are marked with 'o' and '*', respectively and plotted vs the position of the head coil, outside its normal imaging volume.
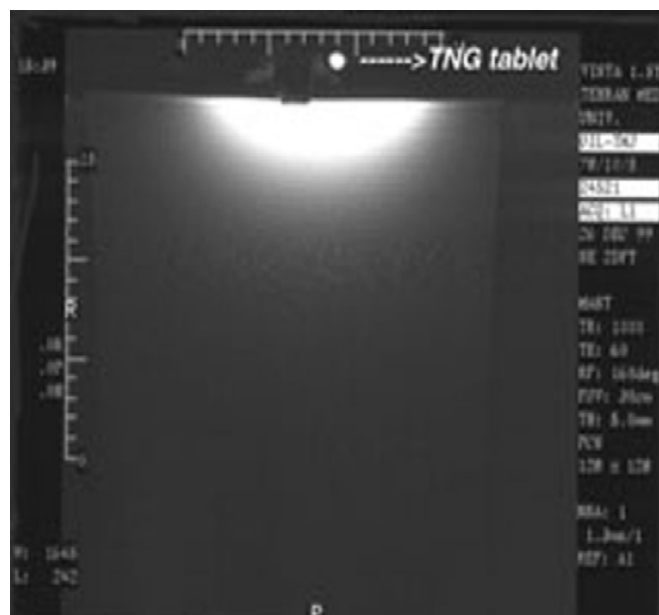
Figure 3: An image of the oil phantom acquired by the TMJ coil. The coil center is marked by a TNG tablet.
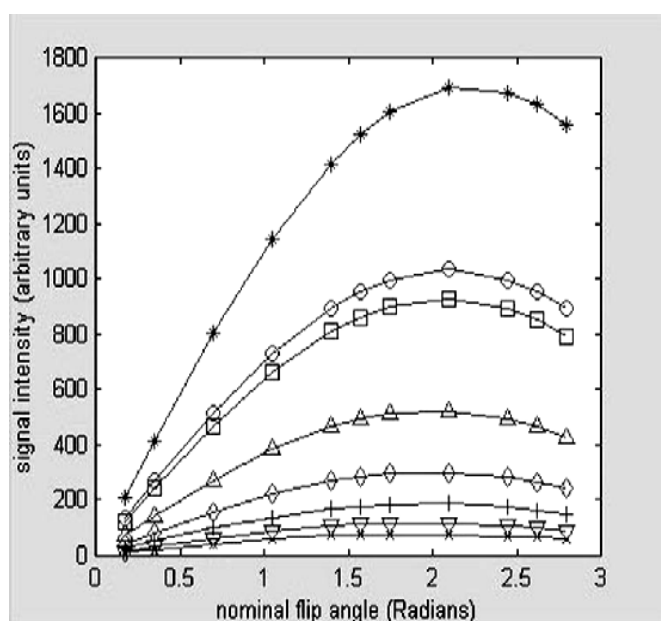
Figure 4: Signal intensity variations vs flip angle for images of the oil phantom acquired by the TMJ coil. The curve which is marked by '*' belongs to the closest ROI to the TMJ coil and the one which is marked by '×' is the farthest away from the TMJ coil.

Figure 5: T(r) for body coil and R(r) for the TMJ coil in A-P direction. T(r) is marked by 'o' and R(r) is marked by '*'.

Conclusion

In this paper a method is introduced, by which the RF transmit and receive uniformity for different coils of an MRI system can be determined using a simple phantom. Our method uses only a routine 0-180° spin echo sequence, needless of any sophisticated protocols. In this pulse sequence, the 180° RF pulse compensates for the dephasing of spins due to Bo non-uniformity. The use of multiple images (eleven for each study) and the curve fitting process improve both the precision and reproducibility of the results. The method is needless of any special hardware or software on MRI scanners and only uses a simple oil phantom. Using an oil phantom has the following advantages: 1) its T_1 is short, thus, short imaging times are achievable without saturation. 2) RF skin depth is long in oil, and therefore, RF pulses penetrate into it easily. 3) RF standing wave is long in oil. The latter two advantages ensure the least interaction between the phantom and RF field, preventing additional RF inhomogeneity.

The θ-2θ pulse sequence that has been used by some other researchers, is not able to compensate for Bo inhomogeneity. In addition, it faces another known problem, that is, the measured points do not match the curve model properly and the best fitted curve does not pass over all data points. This problem is much pronounced when using larger flip angles, as when RF system is functioning outside the range for which it has been designed. Besides, it should be noted that at high RF powers the linear relation between the flip angle and B_1 field intensity does not hold any more. The main drawback of our method is its longer imaging times in comparison to those of the especially designed pulse sequences.[4,15]

By this method, the linear profiles or surface distribution of different coils can be displayed. The method can be considered as a good test for QC of MRI systems, and its results can be used to correct images. The transmitted B_1 field is also measurable *in vivo* by this method.

Appendix

Calculating the Signal Response for the Spin Echo Pulse Sequence

The received MRI signal after applying an RF pulse sequence is proportional to the magnitude of the magnetization vector in the transverse plane. Therefore, for calculating the signal response, we have to calculate the magnitude of the magnetization vector in the transverse plane after the pulse sequence is applied.

The magnetization vector in the steady state is represented by $M_0 = (0, 0, M_0)$. Generally speaking, the magnetization vector is affected by a $\theta x\text{-}\tau\text{-}\alpha y\text{-}\tau$ sequence before the signal is acquired. Where θx is an RF pulse which makes the magnetization vector flip around the x-axis by the value of θ. In the same way, αy is an RF pulse that flips the magnetization vector by the value of α, around the y-axis. τ is the time interval between the two pulses, θx and αy During this time (τ =TE/2) the magnetization vector continues its processional motion around the z-axis with an angular velocity equal to $\Delta\omega$ in the rotating frame of reference. Consequently, the vector M rotates around the z-axis by the value of $\varphi = \Delta\omega . \tau$. So, the magnetization vector first experiences a rotation of θ about x, then φ about z, after that α about y, and finally φ about z axes. To evaluate the final status of the magnetization vector after all these rotations, we must just apply the relevant rotation matrix for each of the rotations of this vector. The magnetization vector, just before acquisition, is calculated as:

$$M_{acq}= R_z(\varphi).R_y(\alpha).R_z(\varphi).R_x(\theta).M_O \qquad (A\text{-}1)$$

Where $R_i(\beta)$ represents a rotation matrix around the axis i by the value β. When M is rotated by value β around an arbitrary axis i, then, its component along this axis remains unchanged. So, for simplicity we consider only a 2×2 rotation matrix for those components that change. If components of the magnetization vector after the first rotation (*i.e.*, θx) are represented as (x_1, y_1, z_1) then we will have:

$$x_1=0$$

$$\begin{bmatrix} y_1 \\ z_1 \end{bmatrix} = \begin{bmatrix} \cos\theta & -\sin\theta \\ \sin\theta & \cos\theta \end{bmatrix} \begin{bmatrix} y_o \\ z_o \end{bmatrix} =$$

$$\begin{bmatrix} \cos\theta & -\sin\theta \\ \sin\theta & \cos\theta \end{bmatrix} \begin{bmatrix} O \\ M_o \end{bmatrix} = \begin{bmatrix} -\sin\theta . & M_o \\ \cos\theta . & M_o \end{bmatrix}$$

Again, if the components of this vector after the second rotation (*i.e.*, φz) are called (x_2, y_2, z_2) then we will have:

$$z_2= z_1= \cos\theta . M_o$$

$$\begin{bmatrix} x_2 \\ y_2 \end{bmatrix} = \begin{bmatrix} \cos\varphi & -\sin\varphi \\ \sin\varphi & \cos\varphi \end{bmatrix} \begin{bmatrix} x_1 \\ y_1 \end{bmatrix} = \begin{bmatrix} \sin\varphi . \sin\theta . M_o \\ -\cos\varphi . \sin\theta . M_o \end{bmatrix}$$

And after the third rotation (αy), we will have:

$$y_3=y_2=-\cos\varphi.\sin\theta.M_O$$

$$x_3=\sin\varphi.\sin\theta.\cos\alpha.M_O-\sin\alpha.\cos\theta.M_O$$

$$z_3=\sin\alpha.\sin\varphi.\sin\theta.M_O+\cos\alpha.\cos\theta.M_O$$

Finally, after φz rotation we will have:

$$z_4=z_3=\sin\alpha.\sin\varphi.\sin\theta.M_O+\cos\alpha.\cos\theta.M_O \quad (A\text{-}2)$$

$$x_4=M_O\left[\tfrac{1}{2}\sin\theta(\cos\alpha+1).\sin2\varphi-\sin\alpha.\cos\theta.\cos\varphi\right] \quad (A\text{-}3)$$

$$y_4=M_O\left[\cos\alpha.\sin\theta.\sin^2\varphi-\cos\theta.\sin\alpha.\sin\varphi-\sin\theta.\cos^2\varphi\right] \quad (A\text{-}4)$$

Considering the uniform distribution of φ in xy plane, the values of M_x and M_y are calculated by integrating equations (A-3) and (A-4) over φ:[16]

$$M_x = \frac{\int_{-\pi}^{\pi} x_4 \cdot d\varphi}{\int_{-\pi}^{\pi} d\varphi} \qquad (A-5)$$

$$M_y = \frac{\int_{-\pi}^{\pi} y_4 \cdot d\varphi}{\int_{-\pi}^{\pi} d\varphi} \qquad (A-6)$$

Therefore:

$$M_x = 0$$

$$M_y = \frac{1}{2} M_0 \sin\theta \cdot (1-\cos\alpha) \quad (A-7)$$

And the magnitude of the transverse magnetization vector is:

$$|M_{xy}|^2 = |M_x|^2 + |M_y|^2 \Rightarrow M_{xy} = \frac{1}{2} M_0 \cdot \sin\theta \cdot (1-\cos\alpha) \quad (A-8)$$

The received signal is proportional to the magnitude of the transverse magnetization vector, thus:

$$SSE \propto \frac{1}{2} M_0 \cdot \sin\theta \cdot (1-\cos\alpha) \quad (A-9)$$

References

1. Velthuizen R et al: Review and evaluation of MRI non-uniformity corrections for brain tumor response measurements. Med Phys 1998; 25(9):1655-1666.
2. Sled JG, Pike GB: Standing wave and RF penetration artifacts caused by elliptic geometry: An electro dynamic analysis of MRI. IEEE Trans Med Imag.1998; 17(4): 653-662.
3. Alsop DC, Connick TJ, Mizsei G: A spiral volume coil for improved RF field homogeneity at high static magnetic field strength. Mag Reson Med1998; 40: 49-54.
4. Stollberger R, Wach P: Imaging of the active B1 field in vivo. Mag Reson Med 1996; 35:, 246-251.
5. Talagala SL, Gillen J.: Experimental determination of three dimensional RF magnetic field distribution of NMR coils. J Mag Reson 1991; 94: 493-500.
6. Boyer JS, Wright SM: An automated measurement system for characterization of RF and gradient coil parameters. J Mag Reson Imag 1998; 8: 740-747.
7. Simmon A, Tofts P, Barker GJ: Sources of intensity non-uniformity in spin echo images at 1.5 T. Mag Reson Med 1994; 32: 121-128.
8. Li S, Yang QX, Smith MB: RF coil optimization of B1 field homogeneity using field histograms and finite element calculations. Mag Reson Imag1994;12(7): 1079-1087.
9. Jin Jianming, Shen G, Perkins T: On the field in-homogeneity of a birdcage coil. Mag Reson *Med*1994; 32: 418-422.
10. Oh CH, Hilal SK, Cho ZH: Radio frequency field intensity mapping using a composite spin echo sequence. Mag Reson Imag 1990; 8: 21-25.
11. Pelnar J: Measurement of the distribution of B1 field in the presence of linear magnetic field gradient. J Mag Reson 1986; 70: 456-460.
12. Jerschow A, Bodenhausen G: Mapping of the B1 field distribution with non-ideal gradients in a high resolution NMR spectrometer. J Mag Reson 1999; 137: 108-115.
13. Insko EK, Bolinger L: Mapping of the radio frequency field. J Mag Reson Series A 1993; 103: 82-85.
14. Barker GJ, Simmons A, Tofts PS: A simple method for investigating the effects of non-uniformity of radio frequency transmission and radio frequency reception in MRI. British Journal of Radiology1998; 71: 59-67.
15. Thulborn Keith R, et al: Correction of B1 inhomogeneities using echo planar imaging of water. Mag Reson Med 1998; 39: 369-375.
16. Zhou, LQ, Zhu YM, Bergot C, et al: A method of radio-frequency inhomogeneity correction for brain tissue segmentation in MRI: Computerized Medical Imaging and Graphics 2001; 25(5): 379-389.
17. Clare S, Alecci M, Jezzard P: Compensating for B1 inhomogeneity using active transmit power modulation, Magnetic Resonance Imaging 2001; 19(10): 1349-1352.
18. Ibrahim, TS, Lee R, Abduljalil AM: Dielectric resonances and B1 field inhomogeneity in UHFMRI: computational analysis and experimental findings. Magnetic Resonance Imaging 2001; 19(2): 219-226.
19. Cassidy PJ, Grieve S, Clarke K, Edwards DJ: Electromagnetic characterisation of MR RF coils using the transmission-line modelling method. Magnetic Resonance Materials in Biology, Physics and Medicine 2002;14(1): 20 – 29.
20. Oghabian MA, Riahi N, Mehdipour Sh: An Investigation on RF Inhomogeneity in MRI When Different Materials Are Scanned. Proceedings of the Second IASTED International Conference, VIIP2002, Sep 2002, Spain: 373-376.